08

Chemiresistive response of SnO_2 thin films to dissociative adsorption of alcohols and ketones

© A.A. Petrunin,[1] O.E. Glukhova[1,2]

[1] Saratov National Research State University,
410012 Saratov, Russia
[2] I.M. Sechenov First Moscow State Medical University,
119048 Moscow, Russia
e-mail: sacha.petrynin@gmail.com

Received December 25, 2024
Revised December 25, 2024
Accepted December 25, 2024

Within the framework of *ab initio* method, a study of the dissociative adsorption process of alcohols (methanol, ethanol, isopropanol, butanol) and ketones (2-octanone, acetone, cyclohexanone, cyclopentanone) on the surface of a thin SnO_2 film was conducted. It was established that the number of hydrogen atoms detached during dissociative adsorption does not significantly affect the binding energy. It was found that dissociative adsorption leads to the emergence of additional peaks in the density of states function in the valence band, which causes hybridization of electron clouds and an increase in resistance. It was demonstrated that the chemiresistive response during dissociative adsorption is, on average, higher for alcohols than for ketones.

Keywords: tin oxide, thin films, DFT method, chemiresistive response, gas sensors, alcohols, ketones.

DOI: 10.61011/TP.2025.05.61126.467-24

Introduction

Creation of a monitoring system capable of determining foreign impurities in the air and its chemical composition became one of the most pivotal issues in today's electronic industry. Although standard analysis methods such as optical spectroscopy and gas chromatography with the use of mass-spectrometers are effective for this purpose, they take a long time to identify the analyte, are expensive, and are not suitable for real-time or in-situ use [1].

In such gas detectors various metal oxides may be used as a sensitive element, e.g. zinc oxide ZnO [2], indium oxide (In_2O_3) [3], gallium oxide (Ga_2O_3) [4] and vanadium boride (V_2O_5) [5]. Yet, tin oxide (SnO_2) is considered one of the most promising materials for gas sensors [6]. This wide-band semiconductor of *n*-type with a band gap of about 3.6 eV stands out for its electrical, optical and chemical stability [7], which makes it promising for use in gas sensors.

As described in papers [8,9], adsorption of analytes on SnO_2 surface is associated with oxygen removal from the thin oxide film which covers pure surface of SnO_2 in the air. At the same time, the analyte interacts with the adsorbing surface via Van der Waals forces, which, largely due to the low binding energy, limits the possible sensitivity of SnO_2 based detectors, but allows it to be used repeatedly. However, in a medium close to vacuum, chemical adsorption prevails, which is characterized by the covalent interaction of the analyte and SnO_2 based detecting surface, and often leads to dissociation of the adsorbed analyte [10–12]. Such a gas detector can only be used once, but its sensitivity is much higher.

In order to explain the patterns in the course of the dissociative reaction, the methods of density functional theory are used (DFT). Thus, in paper [13] it was shown that oxygen vacancies SnO_2 are crucial for the dissociative adsorption of CO molecules on SnO_2 surface. In paper [14], it was revealed that the dissociative adsorption of acetone and ethanol molecules on the surface of SnO_2 is accompanied by charge release, which contributes to a sensitive response of the gas detector. Despite a large number of studies devoted to dissociative adsorption of analytes on the surface of SnO_2 in DFT studies, the nature of sensitivity variation of such sensors remains unclear, since the magnitude of the chemiresistive response (the ratio of the sensor's electrical resistance before and after adsorption) is not calculated.

The purpose of this *ab initio* study is — identification of regularities of changes in the chemiresistive response in SnO_2 gas sensors under associative adsorption of alcohols molecules (methanol, ethanol, isopropanol, butanol) and ketones (2-octanone, acetone, cyclohexanone, cyclopentanone).

1. Research methods

Ab initio computations were carried out using DFT method, realized in the software package Siesta [15]. The exchange-correlation interaction was simulated within generalized gradient approximation (GGA) that was parametrized via Perdew–Burke–Ernzerhof (PBE) [16]. The Grimme correction (DFT-D2) was used to simulate the dissociative adsorption of alcohol and ketone molecules, which implies a long-range dispersion interaction [17,18]. During the study

the full atomic orbital basis set DZP was used, including polarization orbitals with a 600 Ry grid cutting and with $5 \times 5 \times 1$ Monkhorst–Pack set. The non-equilibrium configuration in all computations was searched using Fast Inertial Relaxation Engine (FIRE) [19], the convergence criteria was force value 0.04 eV/Å.

The bond energy was calculated as the difference between total energy E_{total} of „surface + analyte molecule" system and the energies of free analyte E_{mol} and adsorbing surface E_{surf}:

$$E_{bind} = E_{total} - (E_{surf} + E_{mol}). \quad (1)$$

To calculate the chemiresistive response, the surface resistance values SnO_2 were calculated before and after landing of alcohol and ketone molecules. The calculation of electrical conductivity and resistance was implemented using theory of quantum transport, presented in Landauer-Buttiker formalism [20] using non-equilibrium Green-Keldysh functions realized in Transiesta program [21,22]. In this approach, the electrical conductivity is calculated using the formula:

$$G = \frac{e^2}{h} \int_{-\infty}^{\infty} T(E) F_T(E - E_F) dE, \quad (2)$$

where E_F — Fermi energy; e — electron charge; h — Planck constant; F_T — a function that determines thermal broadening of energy levels; $T(E)$ — transmission function. Functions $F_T(E)$ and $T(E)$ depending on the energy of electron states E, are defined by the following expressions:

$$F_T = \frac{1}{4k_B T} \mathrm{sech}^2\left(\frac{E}{2k_B T}\right), \quad (3)$$

$$T(E) = \frac{1}{N} \sum_{k=1}^{N} Tr[\Gamma_s(E) G_C^A(E) \Gamma_D(E) G_C^R(E)], \quad (4)$$

where k_B — Boltzmann constant, $G_C^A(E)$, $G_C^R(E)$ — advanced and retarded Green's function which defines the contact with electrodes; $\Gamma_s(E)$, $\Gamma_D(E)$ source and drain broadening matrices [23]. All resistance analysis was performed using $50 \times 50 \times 1$ Monkhorst–Pack set. N — general number of k-points.

2. Results

To study the dissociative adsorption of alcohols and ketones SnO_2 3D-crystal SnO_2 was selected having a tetragonal crystalline structure ($P4_2/mnm$) with lattice constants $a = b = 4.832$ Å, $c = 3.243$ Å, $\alpha = \beta = \gamma = 90°$. The detecting surface of the periodic thin film SnO_2 was characterized by Miller indices (110) and lattice constants $a = 3.243$ Å, $b = 6.834$ Å, the film thickness was 6.446 Å (cell contains 12 atoms). The sizes of analyte molecules (for example, the area of a cyclopentanone molecule is $\sim 1.791 \times 4.538$ Å) are such that their landing on the surface of the thin film SnO_2 with lattice constants indicated above will inevitably lead to interaction between neighboring molecules. To avoid this, the lattice cell of SnO_2 thin film was enlarged to the supercell $3 \times 2 \times 1$ that contains 72 atoms with lattice constants $a = 9.730$ Å, $b = 13.668$ Å. The supercell SnO_2 and fragment of SnO_2 thin film is given in Fig. 1. The thickness of the thin film didn't change.

The results of dissociative ketone adsorption on the surface of SnO_2 thin film are shown in Fig. 2. As can be seen from the figure, during the dissociative adsorption of 2-octanone and cyclopentanone molecules, 2 hydrogen atoms are separated, whereas during the adsorption of acetone and cyclohexanone — only 1 hydrogen atom. These hydrogen atoms form chemical bonds with the surface of SnO_2 thin film. C–O chemical bonds are also formed between 2-octanone, acetone, and cyclohexanone molecules and SnO_2 surface. It is worth noting that cyclopentanone adsorption occurs without forming C–O bond. The lengths of C–O bonds during ketone adsorption are shown in the table. Dissociation of ketones on the surface of SnO_2 thin film leads to charge transfer between ketones and SnO_2 film. The charge of ketone molecules varies from -0.057e to 0.217e, with the maximum positive charge observed in the cyclohexanone molecule, which is also characterized by the maximum chemical bond length C–O.

Dissociative adsorption of any of the alcohol molecules on the surface of SnO_2 thin film (Fig. 3) occurs with the separation of one hydrogen atom, which chemically binds to SnO_2 thin film. Also, as in the case of ketones, C–O bond is formed between the analyte and the detecting surface. Unlike ketones, all alcohols give a charge to SnO_2 thin film, and the charge value of alcohol molecules varies from 0.126 to 0.205e. On average, alcohols have a charge of $= 0.170$e, while ketones have a charge of $= 0.084$e, which indicates a higher chemiresistive response in alcohols than in ketones.

The table shows the values of the binding energy during dissociative adsorption of alcohols and ketones on the surface of SnO_2 thin film. It is seen that the bond energy, depending on the analyte, takes values from -16.52 to -13.02 eV. Such high modulus values of the bond energy confirm the dissociative nature of adsorption and, as will be seen below, indicate an increase in the resistance of SnO_2 thin film after adsorption of analytes. At the same time, the bond energies of ketones and alcohols do not differ on average. Thus, for ketones, the bond energy is on average $= -14.96$ eV, and for alcohols $= -14.91$ eV. Since all alcohols detach one hydrogen atom during dissociation, and ketones have 1 or 2 hydrogen atoms, it can be concluded that the number of hydrogen atoms that detach during dissociation does not affect the bond energy.

Figure 4 shows the functions of projection density of states (PDOS) during dissociative adsorption of ketone molecules on the surface of SnO_2 thin film. As can be seen from the figure, before ketone adsorption (Fig. 4, a), a significant number of peaks of the density function of states (DOS) of SnO_2 thin films occur in the valence band, i.e. levels below the Fermi level (zero in the graph).

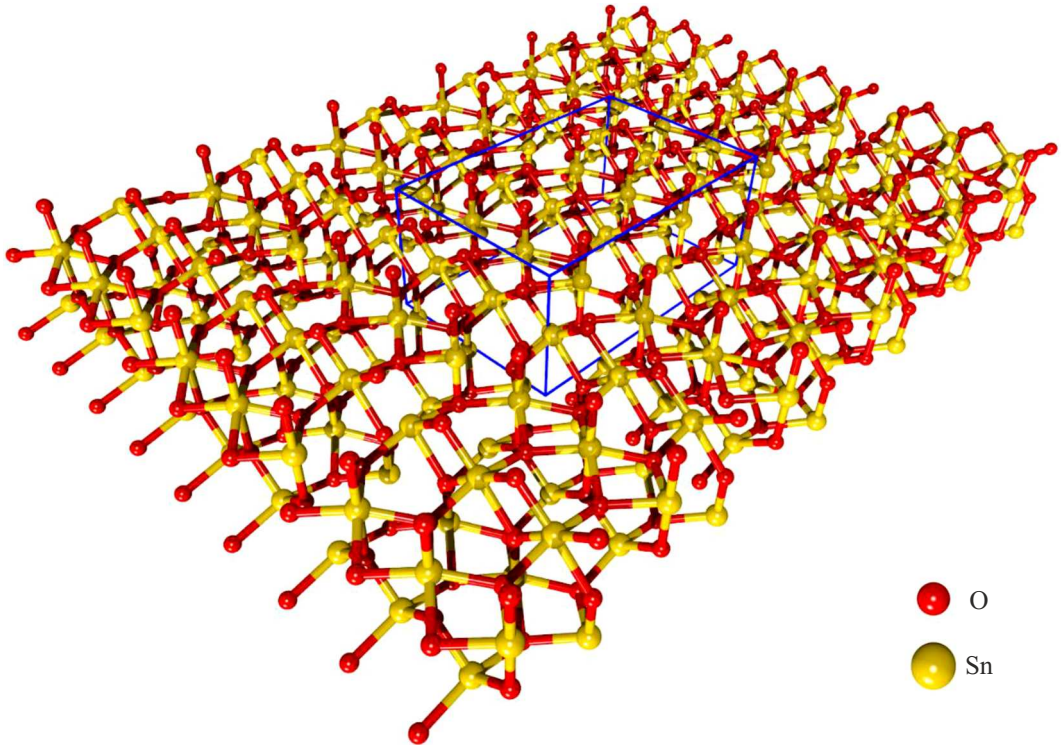

Figure 1. Fragment of SnO_2 thin film with Miller indices (110). A supercell of SnO_2 thin film on which alcohols and ketones were landed is shown inside the rectangular border.

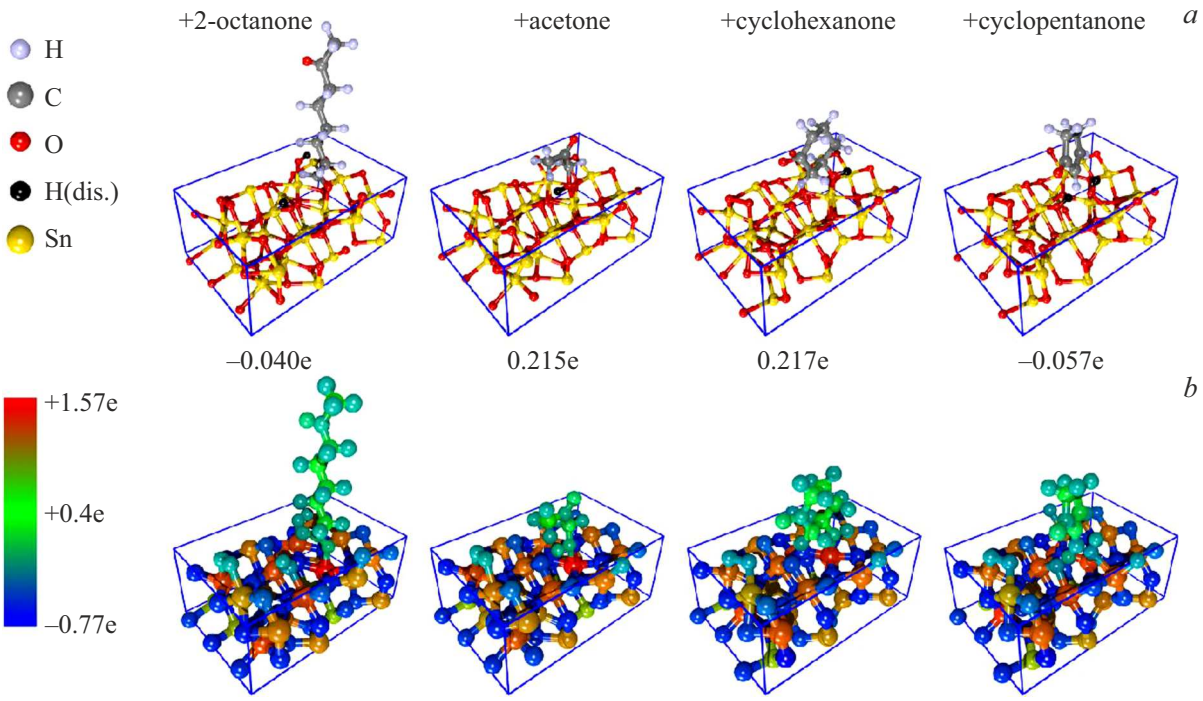

Figure 2. DFT-modeling of the interaction between SnO_2 thin film and ketone molecules (2-octanone, acetone, cyclohexanone, cyclopentanone): *a* — atomistic configurations; *b* — charge distribution (next to each molecule its charge is indicated). Hydrogen atoms detached from ketone molecules due to dissociation are indicated in the figure as H (dis.).

After dissociative adsorption (Fig. 4, *b*–*e*) of ketones the available electronic states of SnO_2 thin film are redistributed and additional DOS peaks appear in the valence band near Fermi level (i.e., in the range from -0.5 to 0.5 eV).

Length of oxygen–carbon bond d(C–O), bond energy E_{bind}, Fermi energy E_F, resistance R and chemiresistive response *Response* of SnO_2 thin films at dissociative adsorption of alcohols and ketones

	d(C–O), Å	E_{bind}, eV	E_F, eV	R, kΩ	*Response*, %
SnO_2	–	–	−7.24	4.20	–
SnO_2 + 2-octanone	1.252	−16.52	−5.53	14.10	335.71
SnO_2 + acetone	1.440	−14.10	−6.06	16.24	386.67
SnO_2 + cyclopentanone	1.496	−14.75	−5.55	76.74	1827.14
SnO_2 + cyclohexanone	–	−14.47	−5.60	67.03	1595.95
SnO_2 + butanol	1.490	−15.68	−5.84	91.66	2182.38
SnO_2 + ethanol	1.444	−16.24	−5.86	15.21	362.86
SnO_2 + isopropanol	1.458	−14.70	−6.27	12.54	298.57
SnO_2 + methanol	1.496	−13.02	−6.43	66.98	1594.76

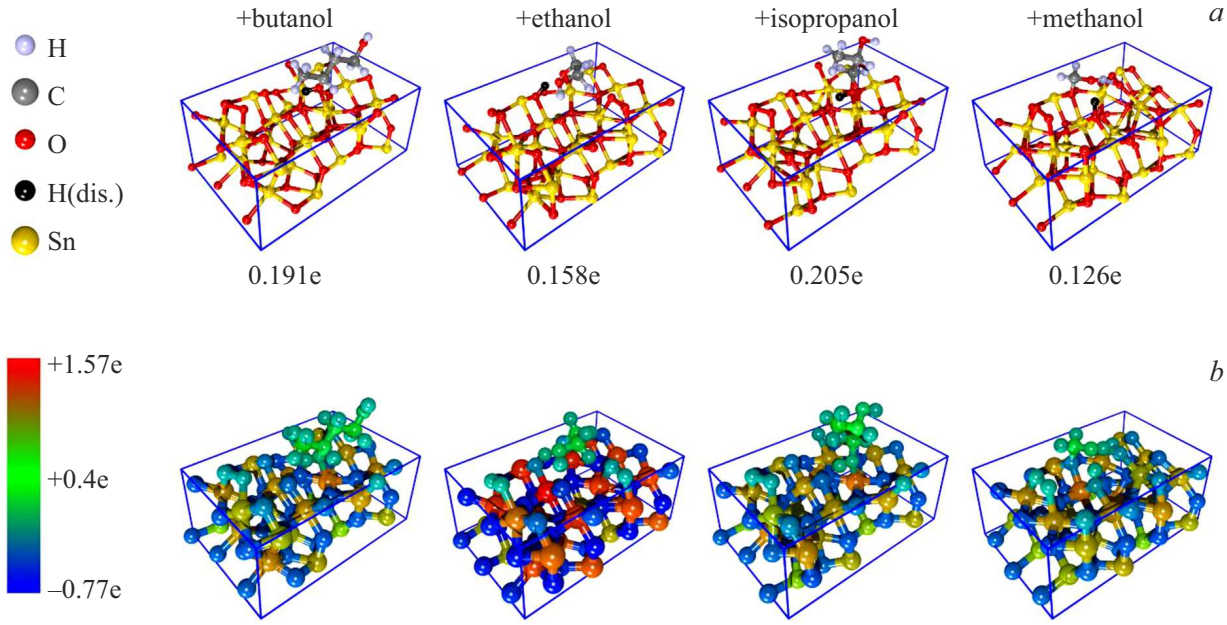

Figure 3. DFT-modeling of the interaction between SnO_2 thin film and alcohol molecules (methanol, ethanol, isopropanol, butanol): *a* — atomistic configurations; *b* — charge distribution (next to each molecule its charge is indicated). Hydrogen atoms detached from alcohol molecules due to dissociation are indicated in the figure as H (dis.).

Thus, during absorption of 2-octanone (Fig. 4, *b*), acetone (Fig. 4, *c*), cyclohexanone (Fig. 4, *d*) and cyclopentanone (Fig. 4, *e*) additonal peaks can be observed on the energy −0.08, −0.01, −0.06 and −0.06 eV respectively. It is worth noting that in all cases, the additional energy levels of ketones fall on the energy levels of thin films SnO_2, which indicates the hybridization of electron orbitals of ketones and SnO_2. Ultimately, such hybridization will lead to higher resistance of SnO_2 thin film with adsorbed alcohol molecules relative to SnO_2 thin film before adsorption and, accordingly, result in higher chemiresistive response.

A similar conclusion can be reached from PDOS analysis of SnO_2 thin film during dissociative adsorption of butanol and ethanol (Fig. 5, *b, c*). Thus, for these molecules, additional peaks in the density of states appear at energies −0.08 and −0.06 eV, respectively. However, during adsorption of isopropanol and methanol, a more significant number of peaks are observed near the Fermi level (i.e., in the range from −0.5 to 0.5 eV). Thus, during isopropanol adsorption, additional peaks (with an intensity greater than 0.1 rel.u.) can be detected at the energy = −0.13, −0.12, −0.11, −0.1, −0.06, −0.05, −0.03 eV. At the same time additional peaks of methanol appear at the energy −0.14, −0.13, −0.12, −0.11, −0.08, −0.02 and 0.00 eV. Such a significant number of peaks in the density function of states for isopropanol and methanol, compared with butanol and ethanol, leads to a change in the electrophysical characteristics of the material and, in particular, lower values of Fermi energy.

Before dissociative adsorption the Fermi energy of thin film SnO_2 = −7.24 eV. After adsorption Fermi energy rises and takes values in the interval from −6.06 (acetone) to −5.53 eV (2-octanone) depending on the landed ke-

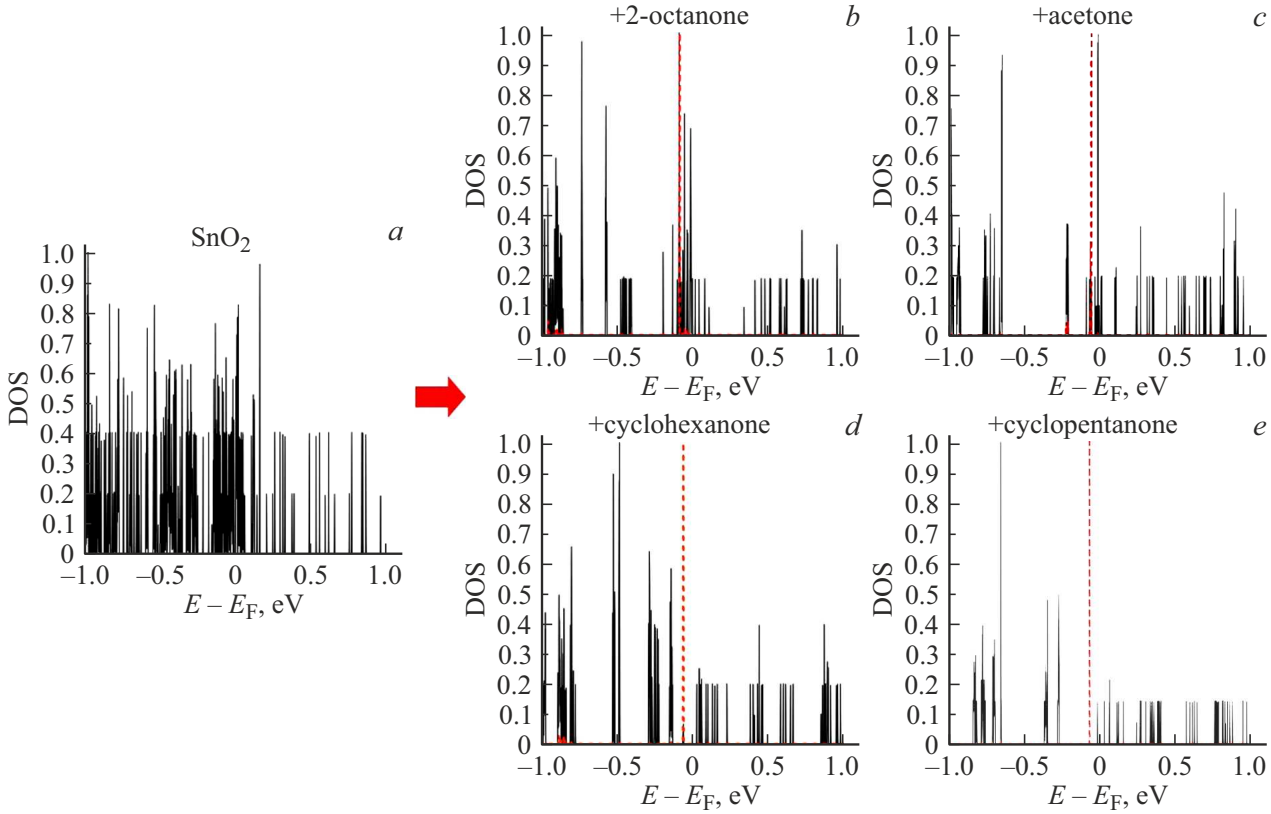

Figure 4. PDOS: *a* — SnO_2 thin film before ketones adsorption; *b* — SnO_2 + 2-octanone system; *c* — SnO_2 + acetone system; *d* — SnO_2 + cyclohexanone system; *e* — SnO_2 + cyclopentanone system. The intensities of peaks are normalized to unity. Fermi level is shifted to zero. Ketone intensity peaks are marked with a dashed line.

tone and from −6.43 (methanol) to −5.84 eV (butanol) depending on the landed alcohol molecule. At the same time, the minimum Fermi energy is observed during the adsorption of isopropanol and methanol. It should be emphasized that Fermi energy is higher for ketones (average Fermi energy = −5.69 eV) than for alcohols (average Fermi energy = −6.10 eV).

Chemiresistive response was found using formula

$$Response = \frac{R_{surf}}{R_{surf+mol}} \cdot 100\,\%,$$

where R_{surf} — resistance of the adsorbing surface SnO_2, $R_{surf+mol}$ — resistance of SnO_2 surface during dissociative adsorption of one of the alcohol molecules (methanol, ethanol, isopropanol, butanol) or ketones (2-octanone, acetone, cyclohexanone, cyclopentanone).

The calculation results are given in the table. As can be seen from the table, the chemiresistive response is on average higher for alcohols (1109.64 %) than for ketones (1036.37 %). It is worth noting that the correlation coefficient of the oxygen-carbon bond length d(C–O) and chemiresistive response $Response = 0.58$, the bond energy E_{bind} and chemiresistive response $Response = 0.29$ and Fermi energy E_F and chemiresistive response $Response = 0.16$, i.e. the correlation of electrophysical parameters with chemiresistive response is small. The main contribution to the change in chemiresistive properties comes from the change of DOS function during dissociative adsorption of analytes, namely, the appearance of additional energy levels of alcohols and ketones, as well as a shift in energy levels SnO_2. Paper [24] presents the results of calculating the chemiresistive response during physical adsorption of alcohols (butanol, ethanol, isopropanol, butanol) and ketones (2-octanone, acetone, cyclopentanone, cyclohexanone) on SnO_2 surface coated with 10 atoms of oxygen, which corresponded to the formation of a thin oxide film on SnO_2 surface in the air. When comparing with results of this work, it can be seen that during physical adsorption on SnO_2 + 10O surface, the chemiresistive response varies in the range from 144.56 % to 188.67 %, while during dissociative adsorption from 298.57 % to 2182.38,% its depends on the analyte. Thus, in the air environment, the formation of a thin oxide film on SnO_2surface leads to a decrease in the chemiresistive response. In addition, as was shown in [25], an increase in temperature reduces the sensitivity of SnO_2 sensors, since fewer molecules form a bond with the detecting surface due to thermal motion.

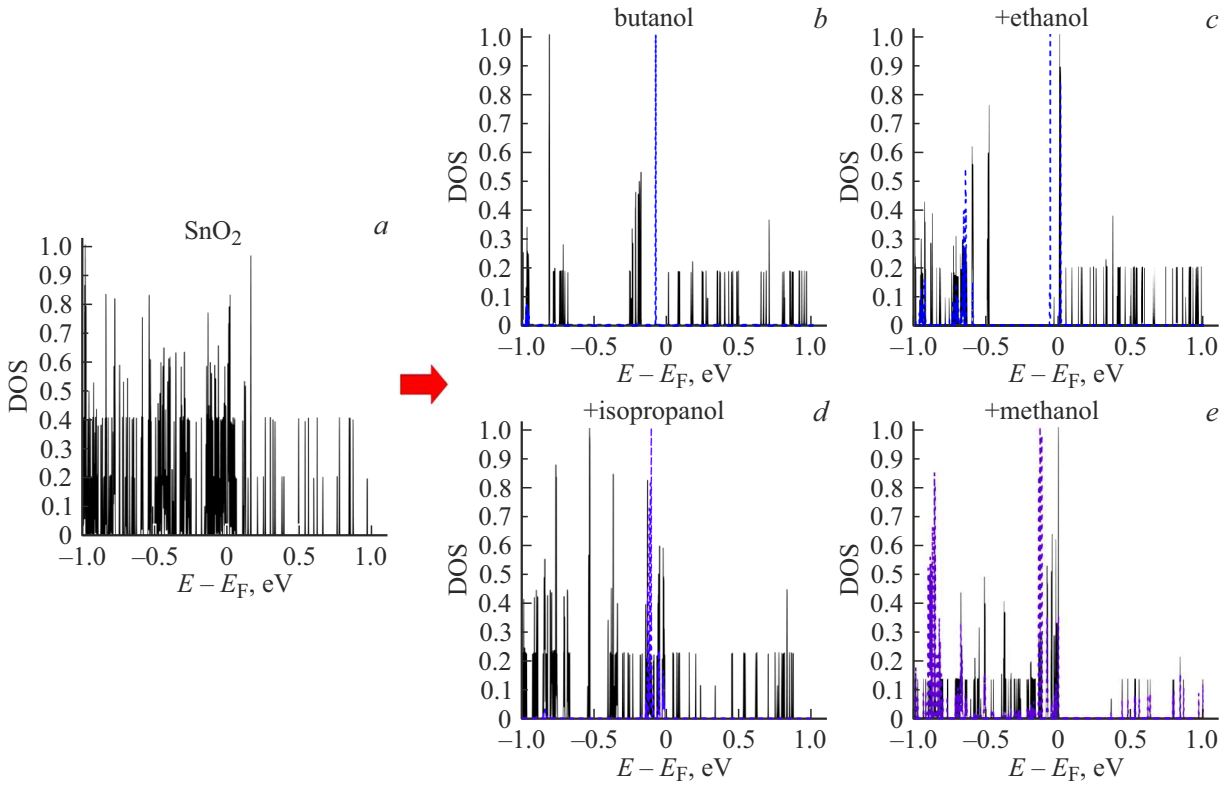

Figure 5. PDOS: *a* — SnO_2 thin film before adsorption of ketones; *b* — SnO_2+ butanol system; *c* — SnO_2 + ethanol system; *d* — SnO_2 + isopropanol system; *e* — SnO_2 + methanol system. The intensities of peaks are normalized to unity. Fermi level is shifted to zero. Alcohols intensity peaks are marked with a dashed line.

Conclusion

In the framework of DFT-studies of dissociative adsorption of alcohols (methanol, ethanol, isopropanol, butanol) and ketones (2-octanone, acetone, cyclohexanone, cyclopentanone) on the surface of SnO_2 thin film, the following main patterns were identified:

1) The number of hydrogen atoms that open during the dissociative adsorption of alcohols and ketones on the surface of SnO_2 thin film has no significant effect on the bond energy. So, on average, the bond energy of ketones differs by 0.33 % from the bond energy of alcohols;

2) dissociative adsorption leads to the appearance of additional peaks of the density function of states mainly in the valence band. These peaks are superimposed on DOS peaks of SnO_2, which leads to hybridization of the electron clouds and an increase in resistance;

3) chemiresistive response during dissociative adsorption is on average by 73.27 % higher for alcohols than for ketones.

Based on the obtained modelling results, it can be concluded that SnO_2 based detectors can find applications in the detection of alcohols and ketones in the near vacuum environment.

Conflict of interest

The authors declare that they have no conflict of interest.

References

[1] S. Dhall, B.R. Mehta, A.K. Tyagi, K. Sood. Sensors Int., **2**, 100116 (2021). https://doi.org/10.1016/j.sintl.2021.100116

[2] K.G. Krishna, G. Umadevi, S. Parne, N. Pothukanuri. J. Mater. Chem. C, **11** (12), 3906 (2023). https://doi.org/10.1039/D2TC04690C

[3] Y. Shi, X. Li, X.F. Sun, X. Shao, H.Y. Wang. J. Alloys Compd., 171190 (2023). https://doi.org/10.1016/j.jallcom.2023.171190

[4] N.N. Yakovlev, A.V. Almaev, V.I. Nikolaev, B.O. Kushnarev, A.I. Pechnikov, S.I. Stepanov, E.V. Chernikov. Mater. Today Commun., **34**, 105241 (2023). https://doi.org/10.1016/j.mtcomm.2022.105241

[5] B.M. Babar, S.H. Sutar, S.H. Mujawar, S.S. Patil, U.D. Babar, U.T. Pawar, P.M. Kadam, P.S. Patil, L.D. Kadam. Mater. Sci. Eng. B, **298**, 116827 (2023). https://doi.org/10.1016/j.mseb.2023.116827

[6] X. Tian, Z. Hu, C. Jia, H. Wang, X. Wei. J. Environ. Chem. Eng., 111516 (2023). https://doi.org/10.1016/j.jece.2023.111516

[7] Y. Masuda. Sens. Actuators B Chem., **364**, 131876 (2022). https://doi.org/10.1016/j.snb.2022.131876

[8] H. Bai, H. Guo, Y. Tan, J. Wang, Y. Dong, B. Liu, Z. Xie, F. Guo, D. Chen, R. Zhang, Y. Zheng. Sens. Actuators B Chem., **340**, 129924 (2021). https://doi.org/10.1016/j.snb.2021.129924
[9] P.G. Choi, N. Izu, N. Shirahata, Y. Masuda. ACS Appl. Nano Mater., **2** (4), 1820 (2019). https://doi.org/10.1021/acsanm.8b01945
[10] J. Zhang, G. Chen, Q. Liu, C. Fan, D. Sun, Y. Tang, H. Sun, X. Feng. Angew. Chem. Int. Ed., **61** (39), e202209486 (2022). https://doi.org/10.1002/anie.202209486
[11] E. Huang, N. Rui, R. Rosales, J. Kang, S. Nemsak, S.D. Senanayake, J.A. Rodriguez, P. Liu. ACS Catal., **12** (18), 11253 (2022). https://doi.org/10.1021/acscatal.2c03060
[12] C. Yang, Z. Li, J. Liu, Y. Zhang, H. Liang, J. Fang, X. Bai, T. Zhao. Mater. Res. Bull., **150**, 111787 (2022). https://doi.org/10.1016/j.materresbull.2022.111787
[13] M. Eslamian, A. Salehi, E. Nadimi. Surf. Sci., **708**, 121817 (2021). https://doi.org/10.1016/j.susc.2021.121817
[14] A.A. Abokifa, K. Haddad, J. Fortner, C.S. Lo, P. Biswas. J. Mater. Chem. A, **6** (5), 2053 (2018). https://doi.org/10.1039/C7TA09535J
[15] J.M. Soler, E. Artacho, J.D. Gale, A. García, J. Junquera, P. Ordejón, D. Sánchez-Portal. J. Phys. Condens. Matter., **14** (11), 2745 (2002). https://doi.org/10.1088/0953-8984/14/11/302
[16] J.P. Perdew, K. Burke, M. Ernzerhof. Phys. Rev. Lett., **77** (18), 3865 (1996). https://doi.org/10.1103/PhysRevLett.77.3865
[17] S. Grimme. J. Comput. Chem., **27** (15), 1787 (2006). https://doi.org/10.1002/jcc.20495
[18] S. Grimme, J. Antony, S. Ehrlich, H. Krieg. J. Chem. Phys., **132** (15), (2010). https://doi.org/10.1063/1.3382344
[19] E. Bitzek, P. Koskinen, F. Gähler, M. Moseler, P. Gumbsch. Phys. Rev. Lett., **97** (17), 170201 (2006). https://doi.org/10.1103/PhysRevLett.97.170201
[20] M. Büttiker, Y. Imry, R. Landauer, S. Pinhas. Phys. Rev. B, **31** (10), 6207 (1985).
[21] M. Brandbyge, J.L. Mozos, P. Ordejón, J. Taylor, K. Stokbro. Phys. Rev. B, **65** (16), 165401 (2002). https://doi.org/10.1103/PhysRevB.65.165401
[22] N. Papior, N. Lorente, T. Frederiksen, A. García, M. Brandbyge. Comput. Phys. Commun., **212**, 8 (2017). https://doi.org/10.1016/j.cpc.2016.09.022
[23] O.E. Glukhova, D.S. Shmygin. Beilstein J. Nanotechnol., **9** (1), 1254 (2018). https://doi.org/10.3762/bjnano.9.117
[24] M.A. Solomatin, M. Radovic, A.A. Petrunin, D.A. Kirilenko, A.S. Varezhnikov, G. Dubourg, M.Yu. Vasilkov, A.M. Bainyashev, A. Nesterovic, I. Kiselev, K.B. Kostin, Yu.P. Martynyuk, A.V. Gorokhovsky, S.S. Volchkov, D.A. Zimnyakov, N.M. Ushakov, V.G. Goffman, M.K. Rabchinskii, O.E. Glukhova, V.V. Sysoev. Chem. Eng. J., **474**, 145934 (2023). https://doi.org/10.1016/j.cej.2023.145934
[25] A.A. Petrunin, O.E. Glukhova. Materials, **16** (1), 438 (2023). https://doi.org/10.3390/ma16010438

Translated by T.Zorina